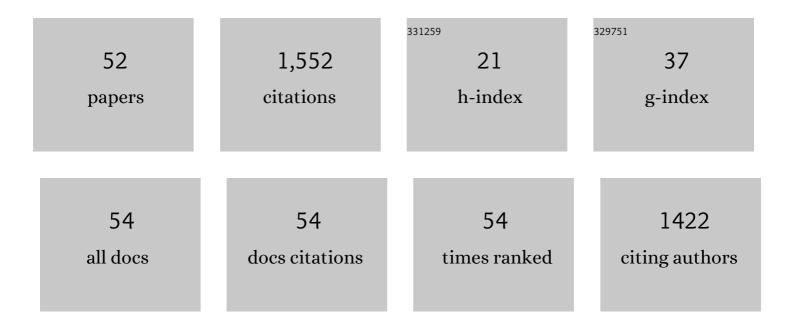
## **Thierry Pourcher**

List of Publications by Year in descending order

Source: https://exaly.com/author-pdf/8540577/publications.pdf Version: 2024-02-01



#	Article	IF	CITATIONS
1	Tumor microenvironment affects exogenous sodium/iodide symporter expression. Translational Oncology, 2021, 14, 100937.	1.7	12
2	Mitotic index determination on live cells from label-free acquired quantitative phase images using a supervised autoencoder. IEEE/ACM Transactions on Computational Biology and Bioinformatics, 2021, 18, 1-1.	1.9	0
3	Quantitative phase microscopy for non-invasive live cell population monitoring. Scientific Reports, 2021, 11, 4409.	1.6	19
4	The PDZ protein SCRIB regulates sodium/iodide symporter (NIS) expression at the basolateral plasma membrane. FASEB Journal, 2021, 35, e21681.	0.2	12
5	Combined Omic Analyzes of Cerebral Thrombi: A New Molecular Approach to Identify Cardioembolic Stroke Origin. Stroke, 2021, 52, 2892-2901.	1.0	10
6	Skin absorption of mixed halide anions from concentrated aqueous solutions. European Journal of Pharmaceutical Sciences, 2021, 166, 105985.	1.9	0
7	Ingested Ketone Ester Leads to a Rapid Rise of Acetyl-CoA and Competes with Glucose Metabolism in the Brain of Non-Fasted Mice. International Journal of Molecular Sciences, 2021, 22, 524.	1.8	17
8	Primal-dual for classification with rejection (PD-CR): a novel method for classification and feature selection—an application in metabolomics studies. BMC Bioinformatics, 2021, 22, 594.	1.2	1
9	Urinary ketone body loss leads to degeneration of brain white matter in elderly SLC5A8-deficient mice. Journal of Cerebral Blood Flow and Metabolism, 2020, 40, 1709-1723.	2.4	6
10	RGD-functionalized magnetosomes are efficient tumor radioenhancers for X-rays and protons. Nanomedicine: Nanotechnology, Biology, and Medicine, 2020, 23, 102084.	1.7	15
11	Comparative analysis of the perception of nuclear risk in two populations (expert/non-expert) in France. Energy Reports, 2020, 6, 2288-2298.	2.5	4
12	Metabolome of Cerebral Thrombi Reveals an Association between High Glycemia at Stroke Onset and Good Clinical Outcome. Metabolites, 2020, 10, 483.	1.3	8
13	Comparison of unsupervised machine-learning methods to identify metabolomic signatures in patients with localized breast cancer. Computational and Structural Biotechnology Journal, 2020, 18, 1509-1524.	1.9	21
14	Proteomic Analysis of Iodinated Contrast Agent-Induced Perturbation of Thyroid Iodide Uptake. Journal of Clinical Medicine, 2020, 9, 329.	1.0	3
15	Improving <sup>131</sup> I Radioiodine Therapy By Hybrid Polymer-Grafted Gold Nanoparticles. International Journal of Nanomedicine, 2019, Volume 14, 7933-7946.	3.3	22
16	LC-MS based metabolomic profiling for renal cell carcinoma histologic subtypes. Scientific Reports, 2019, 9, 15635.	1.6	21
17	A Carboxy-Terminal Monoleucine-Based Motif Participates in the Basolateral Targeting of the Na+/lâ^' Symporter. Endocrinology, 2019, 160, 156-168.	1.4	27
18	Irradiation Effects on Polymer-Grafted Gold Nanoparticles for Cancer Therapy. ACS Applied Bio Materials, 2019, 2, 144-154.	2.3	24

THIERRY POURCHER

#	Article	IF	CITATIONS
19	lodinated Contrast Agents Perturb lodide Uptake by the Thyroid Independently of Free lodide. Journal of Nuclear Medicine, 2018, 59, 121-126.	2.8	13
20	DO MULTIPLE ADMINISTRATIONS OF STABLE IODINE PROTECT POPULATION CHRONICALLY EXPOSED TO RADIOACTIVE IODINE: WHAT IS PRIODAC RESEARCH PROGRAM (2014–22) TEACHING US?. Radiation Protection Dosimetry, 2018, 182, 67-79.	0.4	7
21	Comparison between sparse and concentrated scattering models for characterization of cell-pellet biophantoms and excised mouse tumors. , 2016, , .		Ο
22	A systematic evaluation of sorting motifs in the sodium–iodide symporter (NIS). Biochemical Journal, 2016, 473, 919-928.	1.7	16
23	Single-Photon Emission Computed Tomography for Preclinical Assessment of Thyroid Radioiodide Uptake Following Various Combinations of Preparative Measures. Thyroid, 2016, 26, 1614-1622.	2.4	8
24	Polydisperse structure factor model for understanding the ultrasonic scattering from apoptotic cells. , 2016, , .		1
25	High-Frequency Quantitative Ultrasound Spectroscopy of Excised Canine Livers and Mouse Tumors Using the Structure Factor Model. IEEE Transactions on Ultrasonics, Ferroelectrics, and Frequency Control, 2016, 63, 1335-1350.	1.7	33
26	Evaluation of tetrafunctional block copolymers as synthetic vectors for lung gene transfer. Biomaterials, 2015, 45, 10-17.	5.7	20
27	The sodium/iodide symporter: State of the art of its molecular characterization. Biochimica Et Biophysica Acta - Biomembranes, 2014, 1838, 244-253.	1.4	68
28	99mTcO4â^'-, Auger-Mediated Thyroid Stunning: Dosimetric Requirements and Associated Molecular Events. PLoS ONE, 2014, 9, e92729.	1.1	12
29	Normalisation to Blood Activity Is Required for the Accurate Quantification of Na/I Symporter Ectopic Expression by SPECT/CT in Individual Subjects. PLoS ONE, 2012, 7, e34086.	1.1	10
30	Characterisation of the purified human sodium/iodide symporter reveals that the protein is mainly present in a dimeric form and permits the detailed study of a native C-terminal fragment. Biochimica Et Biophysica Acta - Biomembranes, 2011, 1808, 65-77.	1.4	19
31	Revisiting Iodination Sites in Thyroglobulin with an Organ-oriented Shotgun Strategy. Journal of Biological Chemistry, 2011, 286, 259-269.	1.6	42
32	Distribution and Dynamics of <sup>99m</sup> Tc-Pertechnetate Uptake in the Thyroid and Other Organs Assessed by Single-Photon Emission Computed Tomography in Living Mice. Thyroid, 2010, 20, 519-526.	2.4	33
33	Characterization of small-molecule inhibitors of the sodium iodide symporter. Journal of Endocrinology, 2009, 200, 357-365.	1.2	19
34	Immunoanalysis indicates that the sodium iodide symporter is not overexpressed in intracellular compartments in thyroid and breast cancers. European Journal of Endocrinology, 2009, 160, 215-225.	1.9	40
35	Smallâ€Molecule Inhibitors of Sodium Iodide Symporter Function. ChemBioChem, 2008, 9, 889-895.	1.3	22
36	Comparison of expressed human and mouse sodium/iodide symporters reveals differences in transport properties and subcellular localization. Journal of Endocrinology, 2008, 197, 95-109.	1.2	21

THIERRY POURCHER

#	Article	IF	CITATIONS
37	A 96-Well Automated Radioiodide Uptake Assay for Sodium/Iodide Symporter Inhibitors. Assay and Drug Development Technologies, 2007, 5, 535-540.	0.6	22
38	Expression of the Apical lodide Transporter in Human Thyroid Tissues: A Comparison Study with Other Iodide Transporters. Journal of Clinical Endocrinology and Metabolism, 2004, 89, 1423-1428.	1.8	53
39	Sugar Binding Induced Charge Translocation in the Melibiose Permease fromEscherichia coliâ€. Biochemistry, 2004, 43, 12606-12613.	1.2	27
40	Cytoplasmic Loop Connecting Helices IV and V of the Melibiose Permease from Escherichia coli Is Involved in the Process of Na+-coupled Sugar Translocation. Journal of Biological Chemistry, 2003, 278, 1518-1524.	1.6	25
41	Identification and Characterization of a Putative Human Iodide Transporter Located at the Apical Membrane of Thyrocytes. Journal of Clinical Endocrinology and Metabolism, 2002, 87, 3500-3503.	1.8	142
42	Projection structure at 8 A resolution of the melibiose permease, an Na-sugar co-transporter from Escherichia coli. EMBO Journal, 2002, 21, 3569-3574.	3.5	44
43	Evidence for Intraprotein Charge Transfer during the Transport Activity of the Melibiose Permease fromEscherichia Coliâ€. Biochemistry, 2001, 40, 13744-13752.	1.2	39
44	Phosphorylation of P-glycoprotein by PKA and PKC modulates swelling-activated Cl <sup>â^'</sup> currents. American Journal of Physiology - Cell Physiology, 1999, 276, C370-C378.	2.1	44
45	Membrane Topology of the Melibiose Permease ofEscherichiacoliStudied bymelBâ^'phoAFusion Analysisâ€. Biochemistry, 1996, 35, 4161-4168.	1.2	86
46	Cation and sugar selectivity determinants in a novel family of transport proteins. Molecular Microbiology, 1996, 19, 911-922.	1.2	174
47	Melibiose Permease of Escherichia coli: Substrate-Induced Conformational Changes Monitored by Tryptophan Fluorescence Spectroscopy. Biochemistry, 1995, 34, 6775-6783.	1.2	50
48	Melibiose permease of Escherichia coli: Large scale purification and evidence that H+, Na+, and Li+ sugar symport is catalyzed by a single polypeptide. Biochemistry, 1995, 34, 4412-4420.	1.2	104
49	Melibiose permease of Escherichia coli: Mutation of aspartic acid 55 in putative helix II abolishes activation of sugar binding by Na+ ions. Biochemical and Biophysical Research Communications, 1991, 178, 1176-1181.	1.0	57
50	Melibiose permease and .alphagalactosidase of Escherichia coli: identification by selective labeling using a T7 RNA polymerase/promoter expression system. Biochemistry, 1990, 29, 690-696.	1.2	20
51	Molecular biology and bacterial secondary transportersâ~†. Biochimie, 1989, 71, 969-979.	1.3	9
52	Identification and Characterization of a Putative Human Iodide Transporter Located at the Apical Membrane of Thyrocytes. , 0, .		49